Hindawi
Advances in Materials Science and Engineering
Volume 2017, Article ID 9082164, 8 pages
https://doi.org/10.1155/2017/9082164

Research Article

Preparation of Metal-Containing Diamond-Like Carbon Films by Magnetron Sputtering and Plasma Source Ion Implantation and Their Properties

Stefan Flege,[1] Ruriko Hatada,[1] Andreas Hanauer,[1] Wolfgang Ensinger,[1] Takao Morimura,[2] and Koumei Baba[2,3]

[1]*Department of Materials Science, Technische Universität Darmstadt, Alarich-Weiss-Str. 2, 64287 Darmstadt, Germany*
[2]*Nagasaki University, Graduate School of Engineering, 1-14 Bunkyo, Nagasaki 852-8521, Japan*
[3]*Industrial Technology Center of Nagasaki, Omura, Nagasaki 856-0026, Japan*

Correspondence should be addressed to Stefan Flege; flege@ma.tu-darmstadt.de

Received 6 September 2016; Revised 31 December 2016; Accepted 5 January 2017; Published 23 January 2017

Academic Editor: Hossein Moayedi

Metal-containing diamond-like carbon (Me-DLC) films were prepared by a combination of plasma source ion implantation (PSII) and reactive magnetron sputtering. Two metals were used that differ in their tendency to form carbide and possess a different sputter yield, that is, Cu with a relatively high sputter yield and Ti with a comparatively low one. The DLC film preparation was based on the hydrocarbon gas ethylene (C_2H_4). The preparation technique is described and the parameters influencing the metal content within the film are discussed. Film properties that are changed by the metal addition, such as structure, electrical resistivity, and friction coefficient, were evaluated and compared with those of pure DLC films as well as with literature values for Me-DLC films prepared with a different hydrocarbon gas or containing other metals.

1. Introduction

Diamond-like carbon films offer many advantages such as high hardness and wear resistance, low friction coefficient, low surface roughness, chemical inertness, and optical transparency. Accordingly, DLC is used in a variety of applications such as protection layer on magnetic media, lubricating layer on sliding parts, and coating on biomedical implants, as antireflective coating [1] or diffusion barrier [2]. Disadvantages of DLC are its poor thermal stability [3], high internal stresses which might lead to poor adhesion on some substrates such as steel and copper [4], and an increase of friction coefficient with humidity [5]. Most of those limitations can be circumvented by a modification of the DLC film, that is, by the addition of one or more elements to the film [6]. Apart from a few light elements, for example, B [7], N [8], or F [9], mainly transition metals are added for this purpose [6, 10].

DLC films can be produced by a variety of methods [11], which include plasma source ion implantation (PSII) [12, 13]. This technique makes it possible to coat complex shaped three-dimensional samples homogeneously without the use of sample manipulation [14]. The sample is placed within a plasma and the ions of this plasma are accelerated towards the sample by a negative voltage applied to the sample or to the sample holder. By using a hydrocarbon gas, DLC films can be produced [15]. Usually, a pulsed high voltage is used to avoid excessive heating of the substrate.

The choice of hydrocarbon gas whose molecules (or fragments thereof) will form the DLC layer depends on the desired properties, and thus the application, of the DLC film [16]. Considerations are the implantation depth, the deposition rate, the hydrogen content, and the structure of the DLC film. While small molecules such as methane (CH_4) are the preferred choice for implantation, they tend to provide only low deposition rates. The use of bigger molecules is equivalent to higher deposition rates. To keep the hydrogen content in the DLC film low, usually molecules with a parity or near-parity of the number of C and H atoms are chosen; that is, acetylene (C_2H_2) and toluene (C_7H_8) are commonly

used. A higher hydrogen content will decrease the hardness of the films [17]. Then again, the friction coefficient is generally lower when the hydrogen content is higher [18]. Here, we will show that the use of ethylene (C_2H_4) is a suitable choice for the preparation of DLC films, too.

A metal can be added to the DLC film by sputtering. Magnetron sputter sources are a mature and affordable technology. However, most of the sputtered material is provided in a neutral state [19, 20], provided that no high power impulse sputtering is used [21]. Below, evidence will be provided that in combination with the PSII process some of the sputtered metal atoms are ionized by the plasma and can thus be implanted into the substrate. The combination of a magnetron sputter source with plasma source ion implantation is sometimes called magnetron plasma source ion implantation [22].

When metal sputtering is combined with DLC deposition by PSII, the setup transforms into a reactive sputtering system. Even though argon is commonly used for the sputtering of the metal, the precursor for the DLC film is also in the vacuum chamber at the same time. Hence, the hydrocarbon will deposit onto the sputtering target, too. This leads to target poisoning which reduces the deposition rate of the metal but in turn provides more carbon to the sample. One way to change the amount of metal within the deposited film is to vary the ratio of the flow rates of argon and hydrocarbon gas [23]. As this process also depends on the sputter yield of the metal, the incorporation of different metals into the DLC film requires different preparation parameters. This will be exemplified by the use of copper and titanium.

2. Materials and Methods

In this study, reactive magnetron sputtering with a mixture of Ar and a hydrocarbon gas (C_2H_4) in combination with PSII was used to produce Me-DLC films on silicon wafer and glass substrates. Metal discs were used as targets for the sputter source, which was operated in RF power mode. A negative high voltage pulse was applied to the substrate holder. This voltage was also used to generate the plasma; that is, there was no additional plasma source (apart from the sputter source). The distance between the sputter source and the sample holder was in the range of 10 cm. For a schematic of the setup, see Figure 1. The content of metal was varied by changing the flow rate ratio of Ar and the hydrocarbon gas, that is, retaining an Ar flow rate of 20 sccm and varying the C_2H_4 flow rate, while keeping the same pressure of 0.7 Pa by changing the pumping rate.

The metal content and the distribution with depth were measured by Auger electron spectroscopy (AES) and X-ray photoelectron spectroscopy (XPS). Additional depth profiles were recorded by secondary ion mass spectrometry (SIMS). The structure of the films was investigated by glancing incidence X-ray diffraction (XRD), Raman spectroscopy (514 nm wavelength), and XPS. The electrical resistivity was measured with a four-point probe and the tribological properties with a ball-on-disk setup using a tungsten carbide ball (6 mm diameter, force 1 N, linear speed 10 cm/s, test at room temperature and ~20% relative humidity). The film adhesion was measured with a pull-off test of an Al pin that was glued to the surface by an epoxy resin.

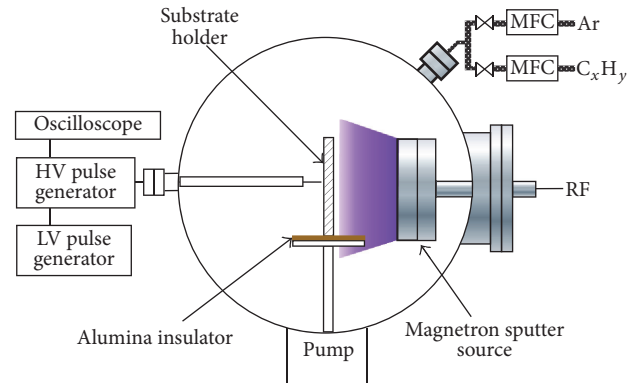

Figure 1: Schematic diagram of the magnetron PSII system. MFC = mass flow controller.

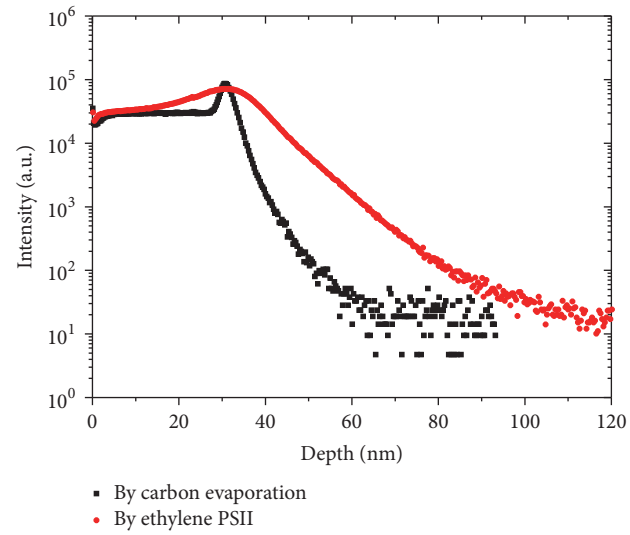

Figure 2: SIMS depth profile of a carbon film, deposited by evaporation (black) and by ethylene PSII at −15 kV (red).

3. Results and Discussion

3.1. Preparation Process and Metal Content. With a combination of sputtering and PSII both parts will influence the film properties.

In accordance with the concept of PSII, ions generated from the surrounding gas are implanted into the substrate. Using exclusively a hydrocarbon gas, some of its molecules will be ionized when the high voltage pulse is applied to the substrate. As a consequence, a DLC film will be deposited on the substrate. With C_2H_4 DLC films can be grown. Figure 2 shows that the carbon from the C_2H_4 is not only deposited onto the substrate, but also implanted into it (process conditions: −15 kV, pulse length 10 μs, and 1 kHz repetition rate). The SIMS depth profile of the carbon shows a slowly declining signal that reaches several ten nm into the silicon substrate. In the case of a carbon film of similar

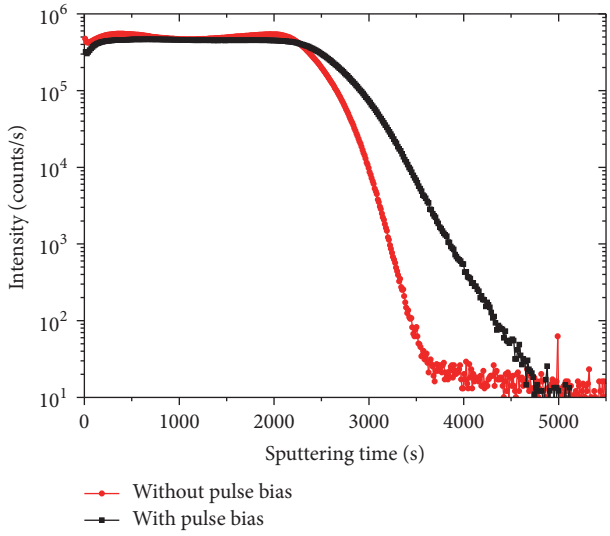

Figure 3: SIMS depth profile of the titanium signal of a sputter deposited Ti film with and without pulse bias.

thickness, which was deposited by evaporation of a carbon thread in a carbon coater, the slope of the signal is much higher.

Adding argon to the plasma gas changes the film structure. Now, not only the hydrocarbon molecules are ionized but also some of the argon atoms. When the argon ions hit the substrate, they will introduce more energy into the film. On the one hand, this leads to a higher disorder within the film caused, for example, by broken bonds. On the other hand, the argon will remove some of the already deposited film by sputtering, thereby decreasing the deposition rate.

Sputtered particles from a magnetron sputter source in proximity of the substrate can be considered to contribute to the gas phase. Hence, at least some of the sputtered particles should be ionized by the plasma from the PSII part of the setup. An easy way to demonstrate this is the preparation of a metal layer on a flat substrate by using only argon as process gas, one time without and one time with pulse bias applied to the sample holder. Depth profiling through the interface of the samples reveals that the interface is wider in the case when a pulse bias is used. In Figure 3 SIMS depth profiles are shown with only the signal of ^{48}Ti of both samples. The wider interface is apparent for the case of the pulse bias (−10 kV with 1 kHz repetition rate and 10 μs pulse length). The metal was implanted into the substrate, even if some part of this wider profile might be attributed to knock-on effects of the argon ions that impinge onto the sample during the high voltage pulse. Because of the metal gradient within the interface the adhesion of the metal layer is higher than in the case of no pulse bias. The adhesion of a sputtered copper film on silicon increases by about 15% when a pulse bias is used, from 29 to 34 MPa.

The second important process is occurring at the sputter source. The main parameter that influences not only the deposition rate of the Me-DLC film but also the metal content within the film is the ratio of the flow rates of the process gases. Usually, the flow rate of argon, which is used for sputtering of the metal target, is much higher than that of the hydrocarbon. Starting with a flow rate of zero for the hydrocarbon, there is obviously only the deposition of metal onto the substrate. Increasing the relative flow of the hydrocarbon to a few percent, there is a sharp decrease in metal content [24]. Because the hydrocarbon in front of the sputter source is ionized in the same way as the argon is, it is also accelerated onto the sputter target. In contrast to argon, the hydrocarbon tends to form a film on the target. Depending on the relative amount of incoming and deposited carbon ions and of the impinging argon ions, the thickness of the carbon film on the target is changed. When the target is completely covered with carbon, no metal will be deposited onto the substrate any more but only carbon which is sputtered from the target. To avoid this, the relative amount of argon is kept high. In Figure 4 the resulting metal contents for Cu and Ti as measured by XPS are presented for different flow rates of C_2H_4 at a fixed flow rate of 20 sccm for Ar. While at 2 sccm of C_2H_4 there is nearly no titanium in the samples because of the target poisoning, there is still about one-third of metal content in the case of copper. These values refer to the surface of the Me-DLC films. The sputter yield of copper is much higher than that of titanium. For argon ions at an energy of 1 keV, the yield is 3.8 for copper but only 0.9 for titanium, according to SRIM [25] simulations. No metal was found in the surface of different metal DLC films when the relative amount of methane in the process gas constituted 25% or more [24]. Here, a similar observation can be made. At above 5 sccm C_2H_4 flow, the copper content in the film is not more than 1 at.%.

Depending on the time scale of the target poisoning, a gradient of the metal can develop during the deposition. At first, that is, near the substrate, the metal content will be high. With time the hydrocarbon deposits onto the target, diminishing the amount of sputtered metal. In Figure 5 SIMS depth profiles of two Cu-DLC films prepared with different flow rates of C_2H_4 and a constant flow rate of 20 sccm of argon are shown. The deposition time was 20 minutes. For the higher metal content, a more or less constant concentration throughout the film was found. Higher flow rates of the hydrocarbon lead to a decrease of the metal content towards the surface. In the case of 6 sccm C_2H_4 flow it can be seen that it takes about 15 minutes until the process of target poisoning is completed. For certain applications this metal gradient might be desirable and can be produced in this way. If a constant metal concentration throughout the film is required, the process should initially be run with a closed shutter in front of the magnetron source and with no high voltage applied to the sample holder until a steady state is reached. The state of the target poisoning can be controlled by means of optical spectrometry [26], for example, provided that there is a line of sight to the plasma in front of the magnetron sputter source.

3.2. Structure of Me-DLC Films. When considering the structural changes within the DLC film, it can be found that the results depend on the type of metal. When a carbide forming metal such as Ti, Ta, W, Mo, or Nb is added in sufficient concentration, small crystalline metal carbide clusters are

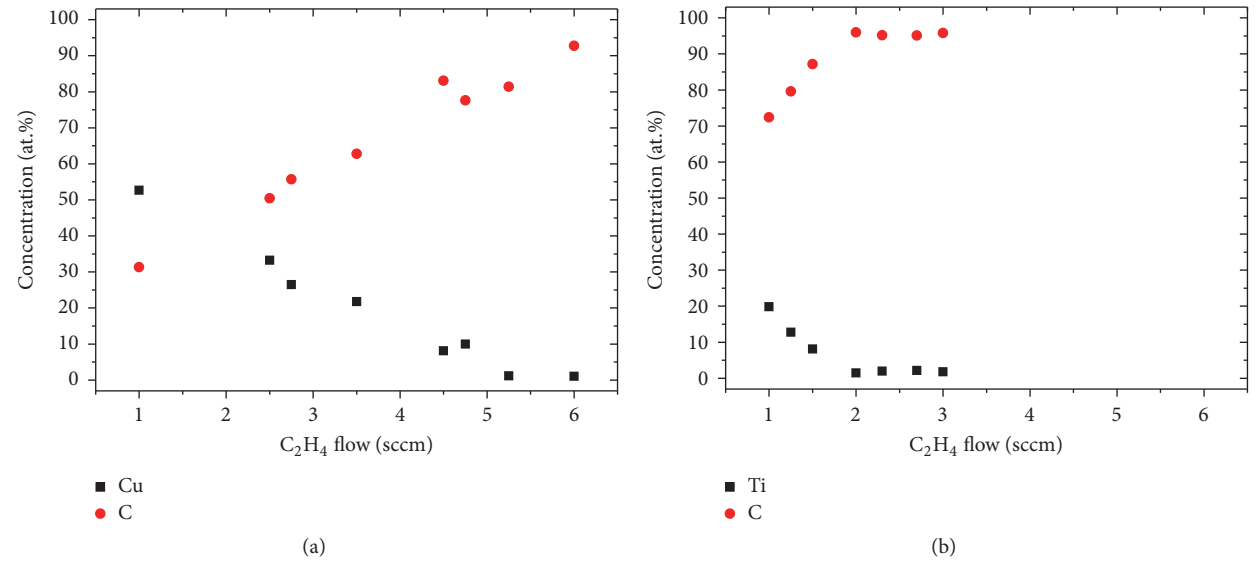

FIGURE 4: Composition of (a) Cu-DLC and (b) Ti-DLC films as a function of C_2H_4 flow rate, with a fixed Ar flow rate of 20 sccm.

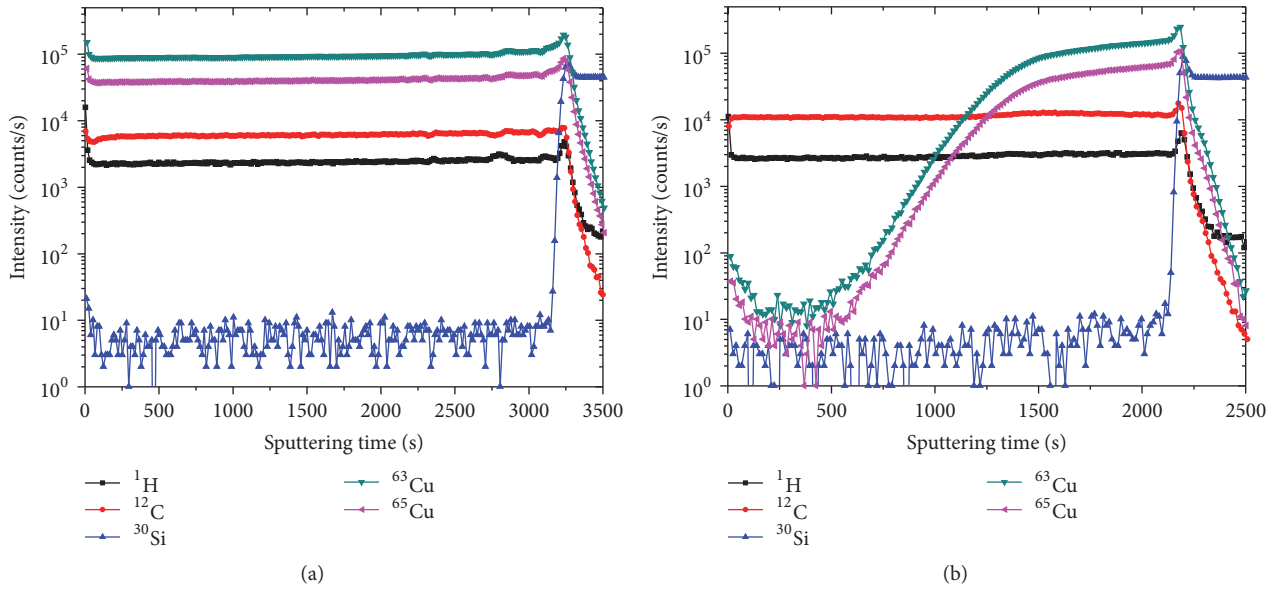

FIGURE 5: SIMS depth profiles of Cu-DLC films prepared by a flow of 20 sccm argon and different C_2H_4 flow rates of (a) 2 sccm and (b) 6 sccm.

formed. While no signal for TiC could be found in XRD diffractograms of our Ti-DLC samples (not shown here), with a maximum Ti content of about 20 at.%, a higher metal concentration leads to signals stemming from the carbide phase. In the case of tungsten, there are two phases involved, that is, the WC and the β-WC_{1-x} phase [27]. In the case of Mo, the carbide phase Mo_3C_2 was detected for Mo concentrations of 11 at.% and above [28]. There is a transition from the metal-containing amorphous phase for low concentrations to the metal carbide phase for higher concentrations.

In XPS spectra of the metal signal, here Ti2p, its position is at the one of the carbide, TiC; see Figure 6(a). The presence of the carbide phase can also be seen for higher metal contents in the C1s signal. For a metal content of about 20 at.% a shoulder in the signal towards lower binding energies can be seen. This feature is absent in the case of smaller metal concentrations, for example, 2 at.% in Figure 6(b). Similar results were found based on Ti-DLC films prepared by C_2H_2 [29]. At around 19 at.% Ti a shoulder in the C1s signal is apparent which indicates the formation of TiC. At higher contents, such as 42 at.%, most of the C1s signal represents TiC, while only a small peak for pure C is left. The binding energy of the Ti2p signal shifts accordingly from the Ti to the TiC position. It was concluded that the amorphous metal-containing DLC phase and carbide nanoparticles coexist in a range of roughly 10–30% metal [22, 28], depending on the type of metal. With Ni, Fe and Co carbides were only observed for metal contents of 60% or more [28]. In the case

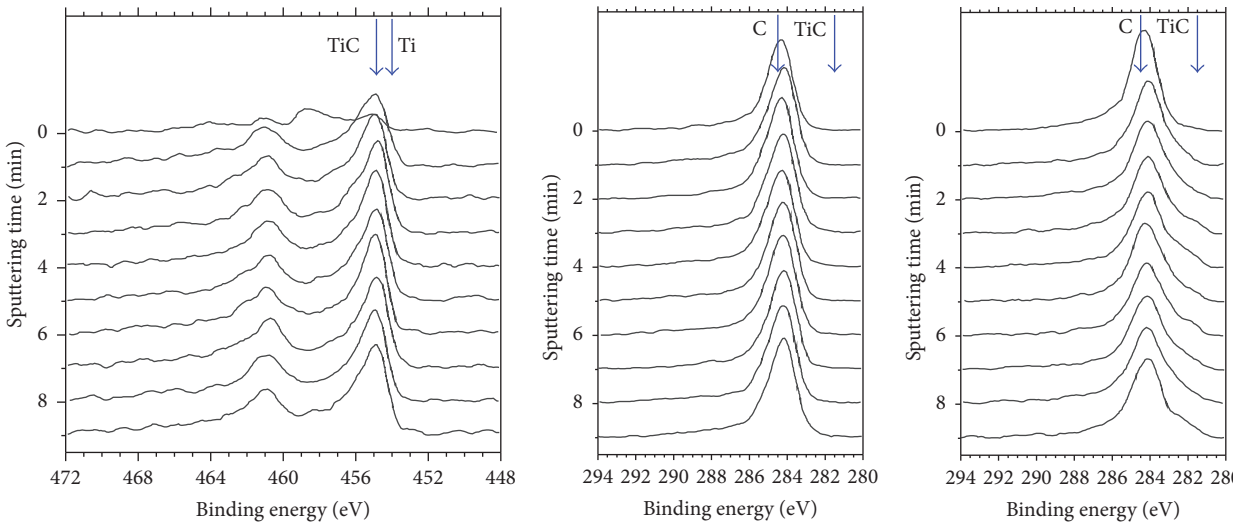

Figure 6: XPS spectra of (a) Ti2p of a Ti-DLC film with about 20 at.% Ti and (b) C1s of Ti-DLC films with 2 at.% (left) and 20 at.% (right) titanium content, respectively.

of copper, the XPS signal positions of C and Cu do not change with metal content (not shown here).

Generally, smaller metal particles within a DLC film are amorphous, whereas larger nanoparticles are of a (poly)crystalline nature [30]. Particle radii increase monotonically with increasing metal content and so do the particle distances [31]. For Nb-DLC and Mo-DLC a crystallite size of 4–6 nm was reported [24]. For Ti-DLC films crystallites of TiC of a similar size (about 10 nm) were found for an amount of 30% of Ti within the films [32]. For Ni the crystalline size was estimated as about 4 nm for a 13% Ni-DLC film [28].

Metals that do not form any carbide, or only weakly, are present as nanocrystalline metal particles within the DLC film. The Ag particles in a film with 3.8 at.% were of several nm size [33]. For copper, nanocrystals with sizes in the range of 15–30 nm were found in samples containing 11–23% Cu [34].

In addition to the formation of carbide, the structure of the carbon film is also affected by the metal incorporation. The films exhibit the two typical features of amorphous carbon films, the D peak around 1350 cm^{-1}, and the G peak in the vicinity of 1550 cm^{-1} [35]. Pure DLC films prepared with C_2H_4 and a pulse voltage of –10 kV possess an intensity ratio of the D peak and the G peak (I_D/I_G) of around 1. This value is a bit higher than the comparison value of 0.86 for films prepared at –10 kV with a pulse of 5 μs length and 1 kHz repetition rate at a pressure of 2 Pa C_2H_2 [36]. Evaluating the hydrogen content of the films by the slope of the luminescence background from the Raman spectra and an empirical formula which links it to the hydrogen content [37], a value of around 30 at.% is derived. This is more than the 26% found for samples made by C_2H_2 [38]; this is expected, however, since the precursor C_2H_4 contains double the amount of hydrogen.

When adding the metal, the I_D/I_G ratio increases, to values of about 1.7 in the case of copper and to values between 2 and 2.5 in the case of titanium. There is no clear dependence on the metal content. The position of the G peak is in the range of 1570 cm^{-1} which indicates, together with the increased intensity ratio and a narrower G peak, an increase of the average crystallite size of sp^2-bonded clusters [11, 37, 39]. Similar observations were made before for carbide formers like Ti [22] and W [27], but also for noncarbide formers like Ag [33].

The ratio of sp^2- and sp^3-bonded carbon is also affected by the incorporation of metal into the film. For vanadium it was found that the ratio shifts from 75 : 25 for a pure DLC film to 38 : 62 for a sample with 48% vanadium carbide and to 20 : 80 for a film with 60% vanadium carbide [40]. In some cases, for example, for copper, an initial reduction of sp^2 content was followed by an increase again with higher copper concentrations [34].

The addition of clusters of metal or metal carbide particles leads to an increase of the surface roughness of the Me-DLC films as compared to pure DLC films. While the latter are generally very smooth with R_a values in the range of 0.1 [41] to 0.2 nm [33], Me-DLC films can exhibit a roughness up to several nm. Ti- and Mo-DLC films seem to be not so rough with values of 0.4 [24] and 0.3–1.1 nm [24, 28], respectively. Nb- and W-DLC films [24] as well as Ni-DLC films [28] can reach several nm of roughness. Especially for metals that tend to form islands when a film is grown, such as silver, the roughness increases with silver content and globular domains can be seen on the film surface [41, 42].

3.3. Electrical Resistivity. Connected with the addition of metal to the DLC film is a drop in electrical resistivity. In Figure 7 this is displayed for the Ti and Cu containing DLC films as a function of the carbon concentration. The starting values for a pure DLC film are around 10 Ωm, which is in the same range as for films prepared by C_2H_2 [22, 29]. With a

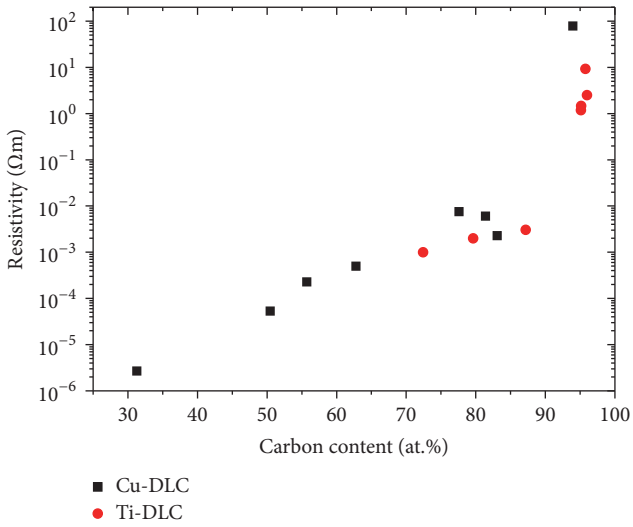

Figure 7: Electrical resistivity of Ti-DLC and Cu-DLC films as a function of the carbon content.

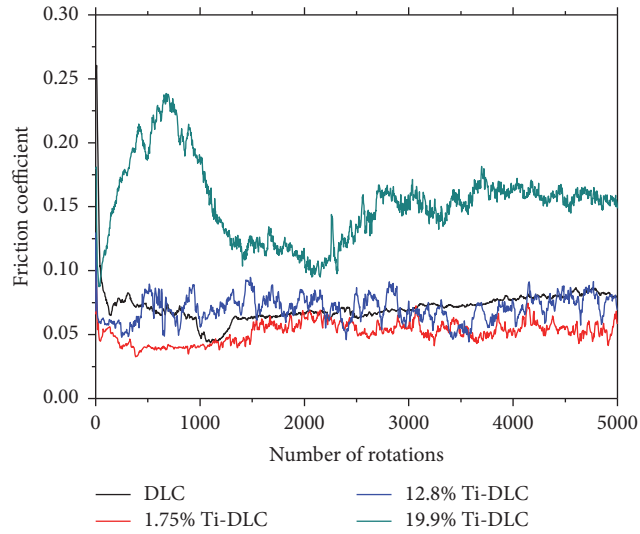

Figure 8: Friction coefficients as a function of number of rotations of Ti-DLC films.

few percent of metal added the resistivity drops sharply. With metal concentrations around 20–25% there is already a drop of about two or three orders of magnitude, which has also been noted for Co and Au additions [43]. When about half of the film consists of metal, the resistivity is merely around 10^{-5} Ωm. From the values in Figure 7 no distinct differences can be seen when comparing Ti- and Cu-DLC films. The decrease of the resistivity with metal content is in most cases nonlinear. This is connected with the structural changes as outlined above and with the changes in the conduction process. With the addition of metal there is a transition from thermally activated conduction along linkages or chains of sp^2 carbon atoms [44] to a process following a percolation law [45]. With metal clusters surrounded by a carbon matrix, there is a combination of percolation and hopping going on. Especially for nickel and iron the different conduction processes lead to a change of electrical resistivity with strain, which can be exploited to manufacture strain sensors [46].

3.4. Tribological Performance. Figure 8 shows the friction coefficient of a pure DLC film and three Ti-DLC films with different Ti contents during a tribology test with a ball-on-disk setup. With a value of 0.05–0.08 the friction coefficient of the pure DLC film is in the same range as the one of the DLC film prepared by C_2H_2 [47]. Even though the film here contains more hydrogen, the difference is apparently not large enough to influence the friction coefficient markedly. With the addition of titanium, the friction coefficient can be decreased. The addition of less than 2 at.% Ti reduces the friction coefficient slightly, to values of around 0.05. A similar effect was reported for Ag-containing films, where 1.8 at.% Ag reduced the friction coefficient to about 0.06 [42]. In case of the Cu-DLC films the friction coefficient of a film with about 1 at.% Cu is similar to the one of the pure DLC film with about 0.06. For a higher Cu content of 9 at.% the friction coefficient is higher, about 0.22.

Values below 0.1 have been reported for other metal-containing DLC films, for example, for 11 at.% Mo [28] and 27 at.% Ta, although there is a large range of Ta content with similar effects [22], and with 9 at.% W [29]. For Ni, Fe, and Co [28] no improvements were found. For Ti-DLC films prepared with C_2H_2 no reduction of the friction coefficient with the addition of Ti was found [29], in contrast to the results reported here.

Factors for the higher friction coefficient with larger amounts of metal are the hardness and the surface roughness. The hardness increases for additions of carbide forming metals, although it takes a volume fraction of about 25% of the metal carbide for distinct changes to be observed [43]. With the addition of noncarbide forming metals, the hardness decreases with metal content, for example, for Ag-DLC films [48, 49]. The surface roughness usually increases with metal content. At low metal contents, small metal precipitates are present, whereas the surface roughness and the hardness are only slightly affected. As a consequence of the nanoscale precipitates [50], the friction coefficient can decrease, as is shown in Figure 8.

The wear of the metal-containing films is slightly higher than that of the pure DLC film. The wear track of the Me-DLC samples after 5000 rotations is about 20–30 nm deep, as measured with a profilometer, with no distinct dependence on metal content. The pure DLC film features a wear track with about 15 nm depth after the test. The higher wear of W containing DLC films was noted before [51].

4. Conclusions

By the use of ethylene gas in combination with reactive magnetron sputtering, metal-containing DLC films can be prepared. The films prepared by C_2H_4 possess a different film structure as compared to ones made by C_2H_2 as evidenced by a higher I_D/I_G ratio and a higher hydrogen content.

The different sputter yields of the metals require different flow ratios of the argon and the hydrocarbon gas to prepare Me-DLC films with similar metal contents. The role of target poisoning of the metal target by the hydrocarbon was exemplarily shown via depth profiles of the Cu-DLC films. The Ti forms carbide within the Ti-DLC films and leads to more distinct changes in the Raman spectra, in contrast to the Cu-DLC films. The effect on the electrical resistivity of the films was similar for both metals, whereas a decrease in friction coefficient could be observed for low content Ti-DLC films and an unchanged friction coefficient for low content Cu-DLC films. Higher metal concentrations lead to a considerably higher friction coefficient, with the value of the Cu-DLC films being higher than the ones of the Ti-DLC films.

Competing Interests

The authors declare that there is no conflict of interests regarding the publication of this paper.

References

[1] A. Grill, "Diamond-like carbon: state of the art," *Diamond and Related Materials*, vol. 8, no. 2-5, pp. 428–434, 1999.

[2] Z. Zhang, R. Song, G. Li, G. Hu, and Y. Sun, "Improving barrier properties of PET by depositing a layer of DLC films on surface," *Advances in Materials Science and Engineering*, vol. 2013, Article ID 861804, 6 pages, 2013.

[3] D. R. Tallant, J. E. Parmeter, M. P. Siegal, and R. L. Simpson, "The thermal stability of diamond-like carbon," *Diamond and Related Materials*, vol. 4, no. 3, pp. 191–199, 1995.

[4] K. C. Walter, M. Nastasi, and C. Munson, "Adherent diamond-like carbon coatings on metals via plasma source ion implantation," *Surface and Coatings Technology*, vol. 93, no. 2-3, pp. 287–291, 1997.

[5] D. Neerinck, P. Persoone, M. Sercu et al., "Diamond-like nanocomposite coatings for low-wear and low-friction applications in humid environments," *Thin Solid Films*, vol. 317, no. 1-2, pp. 402–404, 1998.

[6] J. C. Sánchez-López and A. Fernández, "Doping and alloying effects on DLC coatings," in *Tribology of Diamond-Like Carbon Films*, pp. 311–338, Springer, New York, NY, USA, 2008.

[7] X. Wang and Y. Zhao, "Study of electrical conductivity and microcosmic structure of tetrahedral amorphous carbon films doped by boron," *Advances in Materials Science and Engineering*, vol. 2015, Article ID 727285, 6 pages, 2015.

[8] S. Flege, R. Hatada, M. Hoefling et al., "Modification of diamond-like carbon films by nitrogen incorporation via plasma immersion ion implantation," *Nuclear Instruments and Methods in Physics Research, Section B: Beam Interactions with Materials and Atoms*, vol. 365, pp. 357–361, 2015.

[9] A. Jiang, J. Xiao, X. Li, and Z. Wang, "Effect of structure, composition, and micromorphology on the hydrophobic property of F-DLC film," *Journal of Nanomaterials*, vol. 2013, Article ID 690180, 7 pages, 2013.

[10] A. Markwitz, J. Leveneur, P. Gupta, K. Suschke, J. Futter, and M. Rondeau, "Transition metal ion implantation into diamond-like carbon coatings: development of a base material for gas sensing applications," *Journal of Nanomaterials*, vol. 2015, Article ID 706417, 7 pages, 2015.

[11] J. Robertson, "Diamond-like amorphous carbon," *Materials Science and Engineering: R: Reports*, vol. 37, no. 4–6, pp. 129–281, 2002.

[12] A. Anders, Ed., *Handbook of Plasma Immersion Ion Implantation and Deposition*, John Wiley & Sons, New York, NY, USA, 2000.

[13] J. Pelletier and A. Anders, "Plasma-based ion implantation and deposition: a review of physics, technology, and applications," *IEEE Transactions on Plasma Science*, vol. 33, no. 6, pp. 1944–1959, 2005.

[14] J. R. Conrad, R. A. Dodd, F. J. Worzala, and X. Qiu, "Plasma source ion implantation: a new, cost-effective, non-line-of-sight technique for ion implantation of materials," *Surface and Coatings Technology*, vol. 36, no. 3-4, pp. 927–937, 1988.

[15] J. Chen, J. Blanchard, J. R. Conrad, and R. A. Dodd, "Structure and wear properties of carbon implanted 304 stainless steel using plasma source ion implantation," *Surface and Coatings Technology*, vol. 53, no. 3, pp. 267–274, 1992.

[16] W. Ensinger, "Formation of carbides and diamond-like carbon films by hydrocarbon plasma immersion ion implantation," in *Plasma Surface Engineering Research and Its Practical Applications*, R. Wei, Ed., pp. 135–178, Research Signpost, Trivandrum, India, 2008.

[17] M. Kamiya, H. Tanoue, H. Takikawa, M. Taki, Y. Hasegawa, and M. Kumagai, "Preparation of various DLC films by T-shaped filtered arc deposition and the effect of heat treatment on film properties," *Vacuum*, vol. 83, no. 3, pp. 510–514, 2008.

[18] J. Fontaine, C. Donnet, and A. Erdemir, "Fundamentals of the tribology of DLC coatings," in *Tribology of Diamond-Like Carbon Films*, C. Donnet and A. Erdemir, Eds., pp. 139–154, Springer, Berlin, Germany, 2008.

[19] P. J. Kelly and R. D. Arnell, "Magnetron sputtering: a review of recent developments and applications," *Vacuum*, vol. 56, no. 3, pp. 159–172, 2000.

[20] G. Bräuer, B. Szyszka, M. Vergöhl, and R. Bandorf, "Magnetron sputtering—milestones of 30 years," *Vacuum*, vol. 84, no. 12, pp. 1354–1359, 2010.

[21] K. Sarakinos, J. Alami, and S. Konstantinidis, "High power pulsed magnetron sputtering: a review on scientific and engineering state of the art," *Surface and Coatings Technology*, vol. 204, no. 11, pp. 1661–1684, 2010.

[22] K. Baba and R. Hatada, "Preparation and properties of metal containing diamond-like carbon films by magnetron plasma source ion implantation," *Surface and Coatings Technology*, vol. 158-159, pp. 373–376, 2002.

[23] S. Berg and T. Nyberg, "Fundamental understanding and modeling of reactive sputtering processes," *Thin Solid Films*, vol. 476, no. 2, pp. 215–230, 2005.

[24] C. Corbella, M. Vives, A. Pinyol et al., "Preparation of metal (W, Mo, Nb, Ti) containing a-C:H films by reactive magnetron sputtering," *Surface and Coatings Technology*, vol. 177-178, pp. 409–414, 2004.

[25] J. F. Ziegler, SRIM—The stopping and range of ions in matter, 2013, http://srim.org/.

[26] S. Konstantinidis, F. Gaboriau, M. Gaillard, M. Hecq, and A. Ricard, "Optical plasma diagnostics during reactive magnetron sputtering," in *Reactive Sputter Deposition*, D. Depla and S. Mahieu, Eds., pp. 301–336, Springer, Berlin, Germany, 2008.

[27] K. Baba, R. Hatada, and Y. Tanaka, "Preparation and properties of W-containing diamond-like carbon films by magnetron plasma source ion implantation," *Surface and Coatings Technology*, vol. 201, no. 19-20, pp. 8362–8365, 2007.

[28] K. Baba and R. Hatada, "Preparation and properties of metal-containing diamond-like carbon films by magnetron plasma source ion implantation," *Surface and Coatings Technology*, vol. 196, no. 1–3, pp. 207–210, 2005.

[29] K. Baba and R. Hatada, "Deposition and characterization of Ti- and W-containing diamond-like carbon films by plasma source ion implantation," *Surface and Coatings Technology*, vol. 169-170, pp. 287–290, 2003.

[30] W.-Y. Wu and J.-M. Ting, "Growth and characteristics of carbon films with nano-sized metal particles," *Thin Solid Films*, vol. 420-421, pp. 166–171, 2002.

[31] K. I. Schiffmann, M. Fryda, G. Goerigk, R. Lauer, P. Hinze, and A. Bulack, "Sizes and distances of metal clusters in Au-, Pt-, W- and Fe-containing diamond-like carbon hard coatings: a comparative study by small angle X-ray scattering, wide angle X-ray diffraction, transmission electron microscopy and scanning tunneling microscopy," *Thin Solid Films*, vol. 347, no. 1-2, pp. 60–71, 1999.

[32] A. A. Voevodin, S. V. Prasad, and J. S. Zabinski, "Nanocrystalline carbide/amorphous carbon composites," *Journal of Applied Physics*, vol. 82, no. 2, pp. 855–858, 1997.

[33] K. Baba, R. Hatada, S. Flege et al., "Preparation and antibacterial properties of Ag-containing diamond-like carbon films prepared by a combination of magnetron sputtering and plasma source ion implantation," *Vacuum*, vol. 89, no. 1, pp. 179–184, 2013.

[34] C.-C. Chen and F. C.-N. Hong, "Structure and properties of diamond-like carbon nanocomposite films containing copper nanoparticles," *Applied Surface Science*, vol. 242, no. 3-4, pp. 261–269, 2005.

[35] A. C. Ferrari and J. Robertson, "Interpretation of Raman spectra of disordered and amorphous carbon," *Physical Review B*, vol. 61, no. 20, pp. 14095–14107, 2000.

[36] K. Baba and R. Hatada, "Deposition of diamond-like carbon films on polymers by plasma source ion implantation," *Thin Solid Films*, vol. 506-507, pp. 55–58, 2006.

[37] J. Choi and T. Hatta, "Structural changes of hydrogenated amorphous carbon films deposited on steel rods," *Applied Surface Science*, vol. 357, pp. 814–818, 2015.

[38] R. Hatada, K. Baba, S. Flege, and W. Ensinger, "Long-term thermal stability of Si-containing diamond-like carbon films prepared by plasma source ion implantation," *Surface and Coatings Technology*, vol. 305, pp. 93–98, 2016.

[39] Y. Hirata and J. Choi, "Microstructure of a-C:H films prepared on a microtrench and analysis of ions and radicals behavior," *Journal of Applied Physics*, vol. 118, no. 8, Article ID 085305, 2015.

[40] A. Shigemoto, T. Amano, and R. Yamamoto, "Work function measurements of vanadium doped diamond-like carbon films by ultraviolet photoelectron spectroscopy," https://arxiv.org/abs/1402.1911.

[41] L. Kolodziejczyk, W. Szymanski, D. Batory, and A. Jedrzejczak, "Nanotribology of silver and silicon doped carbon coatings," *Diamond and Related Materials*, vol. 67, pp. 8–15, 2016.

[42] K. Baba, R. Hatada, S. Flege, and W. Ensinger, "Preparation and properties of Ag-containing diamond-like carbon films by magnetron plasma source ion implantation," *Advances in Materials Science and Engineering*, vol. 2012, Article ID 536853, 5 pages, 2012.

[43] C. P. Klages and R. Memming, "Microstructure and physical properties of metal-containing hydrogenated carbon films," *Materials Science Forum*, vol. 52-53, pp. 609–644, 1990.

[44] A. Grill, "Electrical and optical properties of diamond-like carbon," *Thin Solid Films*, vol. 355-356, pp. 189–193, 1999.

[45] R. Sanjinés, M. D. Abad, C. Vâju, R. Smajda, M. Mionić, and A. Magrez, "Electrical properties and applications of carbon based nanocomposite materials: an overview," *Surface and Coatings Technology*, vol. 206, no. 4, pp. 727–733, 2011.

[46] U. Heckmann, R. Bandorf, H. Gerdes, M. Lübke, S. Schnabel, and G. Bräuer, "New materials for sputtered strain gauges," *Procedia Chemistry*, vol. 1, no. 1, pp. 64–67, 2009.

[47] K. Baba, R. Hatada, S. Flege, and W. Ensinger, "Deposition of silicon-containing diamond-like carbon films by plasma-enhanced chemical vapour deposition," *Surface and Coatings Technology*, vol. 203, no. 17-18, pp. 2747–2750, 2009.

[48] H. W. Choi, J.-H. Choi, K.-R. Lee, J.-P. Ahn, and K. H. Oh, "Structure and mechanical properties of Ag-incorporated DLC films prepared by a hybrid ion beam deposition system," *Thin Solid Films*, vol. 516, no. 2-4, pp. 248–251, 2007.

[49] F. R. Marciano, L. F. Bonetti, L. V. Santos, N. S. Da-Silva, E. J. Corat, and V. J. Trava-Airoldi, "Antibacterial activity of DLC and Ag-DLC films produced by PECVD technique," *Diamond and Related Materials*, vol. 18, no. 5–8, pp. 1010–1014, 2009.

[50] C. P. Lungu, "Nanostructure influence on DLC-Ag tribological coatings," *Surface and Coatings Technology*, vol. 200, no. 1–4, pp. 198–202, 2005.

[51] K. Bewilogua, R. Wittorf, H. Thomsen, and M. Weber, "DLC based coatings prepared by reactive d.c. magnetron sputtering," *Thin Solid Films*, vol. 447-448, pp. 142–147, 2004.